mation similar to that assumed in micelles; it is also active and capable of participating in transferring electrons to the lipid phase.

ACKNOWLEDGMENTS

We thank Dr. James W. Whittaker for the use of the Bruker ER 300 spectrometer in his laboratory, Mr. Virgil Simplaceanu for help with the NMR measurements, Dr. Gordon S. Rule for his comments, and Dr. Susan R. Dowd for the synthesis of the spin-labeled lipid and for helpful discussions.

REFERENCES

Arseniev, A. S., Utkin, Y. N., Pashkov, V. S., Tsetlin, V. I., Ivanov, V. T., Bystrov, V. F., & Ovchinikov, Y. A. (1981) *FEBS Lett. 136*, 269-274.

Baldassare, J. J., Robertson, D. E., McAfee, A. G., & Ho, C. (1974) *Biochemistry 13*, 5210-5214.

Barnes, E. M., Jr., & Kaback, H. R. (1971) *J. Biol. Chem. 246*, 5518-5522.

Campbell, H. D., Rogers, B. L., & Young, I. G. (1984) *Eur. J. Biochem. 144*, 367-373.

Chen, K., Morse, P. D., II, & Swartz, H. M. (1988) *Biochim. Biophys. Acta 943*, 477-484.

Ellena, J. F., Archer, S. A., Dominey, R. N., Hill, B. D., & Cafiso, D. S. (1988) *Biochim. Biophys. Acta 940*, 63-70.

Fung, L. W. M., Pratt, E. A., & Ho, C. (1979) *Biochemistry 18*, 317-324.

Futai, M. (1973) *Biochemistry 12*, 2468-2474.

Futai, M. (1974) *Biochemistry 13*, 2327-2333.

Gupta, C. M., Radhakrishnan, R., & Khorana, H. G. (1977) *Proc. Natl. Acad. Sci. U.S.A. 74*, 4315-4319.

Hagen, D. S., Weiner, J. H., & Sykes, B. D. (1979) *Biochemistry 18*, 2007-2012.

Hubbell, W. L., & McConnell, H. M. (1971) *J. Am. Chem. Soc. 93*, 314-326.

Keil, B. (1971) in *The Enzymes, Vol. III, Hydrolysis: Peptide Bonds* (Boyer, P. D., Ed.) 3rd ed., pp 249-275, Academic Press, New York.

Kohn, L. D., & Kaback, H. R. (1973) *J. Biol. Chem. 248*, 7012-7017.

Kovatchev, S., Vaz, W. L. C., & Eibl, H. (1981) *J. Biol. Chem. 256*, 10369-10374.

Matsushita, K., & Kaback, H. R. (1986) *Biochemistry 25*, 2321-2327.

McConnell, H. M. (1976) in *Spin Labeling Theory and Applications* (Berliner, L. J., Ed.) pp 525-560, Academic Press, New York.

Peersen, O., Pratt, E. A., Truong, H.-T. N., Ho, C., & Rule, G. S. (1990) *Biochemistry 29*, 3256-3262.

Pratt, E. A., Jones, J. A., Cottam, P. F., Dowd, S. R., & Ho, C. (1983) *Biochim. Biophys. Acta 729*, 167-175.

Ramachandran, C., Pyter, R. A., & Mukerjee, P. (1982) *J. Phys. Chem. 86*, 3198-3205.

Reeves, J. P., Hong, J.-S., & Kaback, H. R. (1973) *Proc. Natl. Acad. Sci. U.S.A. 70*, 1917-1921.

Rule, G. S., Pratt, E. A., Chin, C. C. Q., Wold, F., & Ho, C. (1985) *J. Bacteriol. 161*, 1059-1068.

Rule, G. S., Pratt, E. A., & Ho, C. (1987a) in *Membrane Proteins* (Goheen, S. C., Ed.) pp 3-20, Bio-Rad Laboratories, Richmond, CA.

Rule, G. S., Pratt, E. A., Simplaceanu, V., & Ho, C. (1987b) *Biochemistry 26*, 549-556.

Shobha, J., Srinivas, V., & Balasubramanian, D. (1989) *J. Phys. Chem. 93*, 17-20.

Short, S. A., Kaback, H. R., & Kohn, L. D. (1974) *Proc. Natl. Acad. Sci. U.S.A. 71*, 1461-1465.

Mechanisms for the Facilitated Diffusion of Substrates across Cell Membranes†

Anthony Carruthers

Department of Biochemistry and Molecular Biology and Program in Molecular Medicine, University of Massachusetts Medical Center, 373 Plantation Street, Worcester, Massachusetts 01605

Received August 24, 1990; Revised Manuscript Received January 10, 1991

ABSTRACT: Two classes of theoretical mechanisms for protein-mediated, passive, transmembrane substrate transport (facilitated diffusion) are compared. The simple carrier describes a carrier protein that exposes substrate influx and efflux sites alternately but never both sites simultaneously. Two-site models for substrate transport describe carrier proteins containing influx and efflux sites simultaneously. Velocity equations describing transport by these mechanisms are derived. These equations take the same general form, being characterized by five experimental constants. Simple carrier-mediated transport is restricted to hyperbolic kinetics under all conditions. Two-site carrier-mediated transport may deviate from hyperbolic kinetics only under equilibrium exchange conditions. When both simple- and two-site carriers display hyperbolic kinetics under equilibrium exchange conditions, these models are indistinguishable by using steady-state transport data alone. Seven sugar transport systems are analyzed. Five of these systems are consistent with both models for sugar transport. Uridine, leucine, and cAMP transport by human red cells are consistent with both simple- and two-site models for transport. Human erythrocyte sugar transport can be modeled by simple- and two-site carrier mechanisms, allowing for compartmentalization of intracellular sugars. In this instance, resolution of the intrinsic properties of the human red cell sugar carrier at 20 °C requires the use of submillisecond transport measurements.

Several fundamental properties of facilitated diffusion (passive transport) systems remain to be resolved. The most basic of these is an understanding of the catalytic principles involved in substrate transport. A detailed knowledge of intermediate forms of carrier/substrate complexes is unavailable, and the physical mechanism(s) by which the carrier protein translocates bound substrate to the opposite side of the mem-

† This work was supported by National Institutes of Health Grant DK 36081.

0006-2960/91/0430-3898$02.50/0

Table I: Solutions to Simple and Two-Site Carrier Models for Transport

$$v_{12} = \frac{S_1(K + S_2)}{K^2R_{oo} + KR_{12}S_1 + KR_{21}S_2 + R_{ee}S_1S_2} \quad (7)$$

constant[a]	simple carrier[b]	iso-two-site carrier[c]	allosteric two-site carrier[d]
K	$\frac{K_2k_{-0}}{k_{-1}} = \frac{K_1k_0}{k_1}$	$\frac{K_2K_7K_8(K_3k_0k_1 + K_1k_2k_0)}{K_3(K_2K_8k_{-0}k_3 + K_1K_7k_0k_{-3})}$	$\frac{K_2K_7K_8(K_3k_1 + K_1k_2)}{K_3(K_2K_8k_3 + K_1K_7k_{-3})}$
nR_{oo}	$\frac{1}{k_{-0}} + \frac{1}{k_0}$	$\frac{(k_0 + K_{-0})\left(\frac{k_0k_{-3}}{K_2K_8} + \frac{k_{-0}k_3}{K_1K_7}\right)}{\left(\frac{k_0k_2}{K_3} + \frac{k_{-0}k_1}{K_1}\right)^2}$	$\frac{2K_1K_3^2k_3}{K_7(K_3k_1 + K_1k_2)^2}$
nR_{12}	$\frac{k_{-0} + k_1}{k_{-0}k_1}$	$\frac{K_1k_0 + K_3k_{-0}}{K_3k_{-0}k_1 + K_1k_0k_2}$	$\frac{K_1 + K_3}{K_3k_1 + K_1K_2}$
nR_{21}	$\frac{k_0 + k_{-1}}{k_0k_{-1}}$	$\frac{K_2k_{-0} + K_4k_0}{K_4k_0k_{-2} + K_2k_{-0}k_{-1}}$	$\frac{K_2 + K_4}{K_4k_{-1} + K_2k_{-2}}$
nR_{ee}	$\frac{k_{-1} + k_1}{k_{-1}k_1}$	$\frac{K_1K_7k_0 + K_2K_8k_{-0}}{K_2K_8k_{-0}k_3 + K_1K_7k_0k_{-3}}$	$\frac{1}{2k_3} + \frac{1}{2k_{-3}}$
constraints	$k_1k_{-0}K_2 = k_{-1}k_0K_1$	$k_{-0}k_1K_2 = k_0k_{-1}K_1$ $k_0k_2K_4 = k_{-0}k_{-2}K_3$ $k_1k_{-3}K_7 = k_{-1}k_3K_8$ $k_{-0}k_3K_2K_8 = k_0k_{-3}K_1K_7$ $k_1k_2K_2K_4 = k_{-1}k_{-2}K_1K_3$	$k_1K_2 = k_{-1}K_1$ $k_2K_4 = k_{-2}K_3$ $k_3K_2K_8 = k_{-3}K_1K_7$

[a] Constants refer to the parameters shown in velocity equation 7. [b] See Figure 1 for interpretation of dissociation and rate constants. [c] See Figure 2 for interpretation of dissociation and rate constants. [d] See Figure 3 for interpretation of dissociation and rate constants.

brane is unknown. In the absence of chemically defined intermediates, most studies have focused upon kinetic analyses of transport. With this approach it is possible to construct models for transport and then to compare experimental and predicted transport behavior. In this way a number of potential transport mechanisms may be rejected.

It seems probable that these carrier systems do not behave as simple, transmembrane pores or channels because many facilitated diffusion systems display the phenomenon of transacceleration. Unidirectional, labeled substrate uptake or efflux is stimulated by the presence of unlabeled substrate at the opposite, trans side of the membrane. This behavior is incompatible with that of membrane channels (Lieb & Stein, 1974a).

This property and other properties of facilitated diffusion systems have led to the highly successful postulate that the carrier proteins exist in two conformational states: their binding sites for substrates are alternately exposed first at one and then the other face of the membrane (Widdas, 1952). This model is generally termed the simple carrier mechanism (Lieb & Stein, 1974b). An alternate view is that these carrier proteins contain multiple, nonexclusive catalytic sites which interact with varying degrees of cooperativity (Baker & Widdas, 1973; Naftalin & Holman, 1977; Holman, 1980).

In this study we compare the predicted behavior of the simple carrier with that of two forms of carrier containing two nonexclusive substrate binding sites (two-site carriers). Previous analyses of two-site carrier mechanisms (Baker & Widdas, 1973; Naftalin & Holman, 1977; Deves & Krupka, 1978; Helgerson & Carruthers, 1989) have presumed that exchange transport is mediated by the simultaneous exchange of two substrate molecules within a single internal carrier pore. In this study we describe two-site carrier exchange transport as coupled movements of substrate through separate carrier subunits. Thus the two-site carrier could be a dimer of two identical simple carriers whose substrate binding sites are arranged in an antiparallel fashion but where isomerization of one subunit promotes the complementary isomerization of the second. More importantly, previous studies made the simplifying assumption of a single, central ternary complex of carrier/extracellular substrate/intracellular substrate. The current study avoids the use of this simplifying assumption.

We show that the steady-state transport properties of these different transport models are quantitatively indistinguishable provided that certain conditions are satisfied. Sugar transport by invertebrate muscle and nerve, by rat hepatocytes and adipocytes, and by rabbit erythrocytes and human erythrocyte leucine, uridine, and cAMP transport are consistent with both the simple and two-site carrier mechanisms. We conclude that for these transport systems the steady-state substrate transport data alone cannot be used to define the formal, kinetic mechanism of transport. Sugar transport in human erthrocytes appears to be incompatible with both classes of carrier mechanism.

Theory

The Simple Carrier. The simple carrier is shown in schematic and King–Altman forms in Figure 1, panels A and B, respectively. We assume that all substrate binding steps are rapid with respect to translocation steps (Lowe & Walmsley, 1986). As transport is passive, the following relationship must hold true:

$$k_{-0}k_1K_2 = k_0k_{-1}K_1$$

Tables I and II summarize the solution to this transport model.

Two-Site Carriers. (A) An Iso-Two-Site Carrier. A theoretical transporter containing simultaneously existent, cis–trans substrate binding sites is shown in Figure 2A. Here, the carrier always presents a substrate efflux and a substrate influx site to the surrounding media. Two forms of unoccupied carrier are possible, and these states isomerize at rates described by the first-order rate constants k_0 and k_{-0}. Exchange transport does not involve simultaneous movements of sugar molecules through a single cavity. Each substrate molecule

Table II: Interpretation of Experimental Michaelis and Velocity Parameters

procedure[a]	simple carrier[b]	iso-two-site carrier[c]	allosteric two-site carrier[d]
zero trans[e]	$V_{12}^{zt} = \frac{1}{R_{12}} \quad K_{12}^{zt} = \frac{KR_{oo}}{R_{12}} \quad \pi = \frac{1}{KR_{oo}}$	identical with simple carrier	identical with simple carrier
	$V_{21}^{zt} = \frac{1}{R_{21}} \quad K_{21}^{zt} = \frac{KR_{oo}}{R_{21}} \quad \pi = \frac{1}{KR_{oo}}$		
infinite cis[f]	$V_{12}^{ic} = \frac{1}{R_{12}} \quad K_{12}^{ic} = \frac{KR_{12}}{R_{ee}}$	identical with simple carrier	identical with simple carrier
	$V_{21}^{ic} = \frac{1}{R_{21}} \quad K_{21}^{ic} = \frac{KR_{21}}{R_{ee}}$		
infinite trans[g]	$V_{12}^{it} = \frac{1}{R_{ee}} \quad K_{12}^{it} = \frac{KR_{21}}{R_{ee}} \quad \pi = \frac{1}{KR_{21}}$	identical with simple carrier	identical with simple carrier
	$V_{21}^{it} = \frac{1}{R_{ee}} \quad K_{21}^{it} = \frac{KR_{12}}{R_{ee}} \quad \pi = \frac{1}{KR_{12}}$		
equilibrium exchange[h]	$V_{12}^{ee} = V_{21}^{ee} = \frac{1}{R_{ee}} \quad \pi = \frac{1}{KR_{oo}}$	$V_{12}^{ee} + V_{21}^{ee} = \frac{1}{R_{ee}} \quad \pi = \frac{1}{KR_{oo}}$	$V_{12}^{ee} = V_{21}^{ee} = \frac{1}{R_{ee}} \quad \pi = \frac{1}{KR_{oo}}$
	$K_{12}^{ee} = K_{21}^{ee} = \frac{KR_{oo}}{R_{ee}} = K_{0.5}^{ee}$	when $R_{oo} = R_{12} + R_{21} - R_{ee}$, $K_{0.5}^{ee} = \frac{KR_{oo}}{R_{ee}}$	when $R_{oo} = R_{12} + R_{21} - R_{ee}$, $K_{0.5}^{ee} = \frac{KR_{oo}}{R_{ee}}$
	$K_{0.5}^{ee} = \frac{-K\left(2 - \frac{R_{12}+R_{21}}{R_{ee}}\right) + \left[K_2\left(2 - \frac{R_{12}+R_{21}}{R_{ee}}\right)^2 + \frac{4K^2R_{oo}}{R_{ee}}\right]^{1/2}}{2}$		
constraints	$R_{12} + R_{21} = R_{oo} + R_{ee}$		

[a] Title of experimental procedure. [b] The model shown in Figure 1. [c] The model shown in Figure 2. [d] The model shown in Figure 3. [e] The zero-trans procedure. Uptake: S_2 is varied, $S_1 = 0$. V_{max} for uptake of S_2 is V_{21}^{zt}. $K_{m(app)}$ for uptake of S_2 is K_{21}^{zt}. Efflux: $S_2 = 0$, S_1 is varied. V_{max} for efflux of $S_1 = V_{12}^{zt}$. $K_{m(app)}$ for efflux of $S_1 = K_{12}^{zt}$. [f] The infinite-cis procedure. Uptake: S_2 is saturating, S_1 is varied. V_{max} for uptake of S_2 is $V_{21}^{ic} = V_{21}^{zt}$. $K_{m(app)}$ for exit of S_1 is K_{21}^{ic}. Efflux: S_2 is varied, S_1 is saturating. V_{max} for efflux of $S_1 = V_{12}^{ic} = V_{12}^{zt}$. $K_{m(app)}$ for uptake of $S_2 = K_{12}^{ic}$. [g] The infinite-trans procedure. Uptake: S_2 is varied, S_1 is saturating. Unidirectional uptake of labeled S_2 is measured. V_{max} for uptake of S_2 is V_{21}^{it}. $K_{m(app)}$ for uptake of S_2 is K_{21}^{it}. Efflux: S_2 is saturating, S_1 is varied. Unidirectional efflux of labeled S_1 is measured. V_{max} for efflux of $S_1 = V_{12}^{it}$. $K_{m(app)}$ for exit of $S_1 = K_{12}^{it}$. [h] The equilibrium exchange condition. $S_1 = S_2$ = varied. Unidirectional uptake or efflux of labeled S is measured. V_{max} for uptake/efflux = V^{ee}. $K_{m(app)}$ for hyperbolic uptake/efflux = K^{ee}. [i] This equation applies to all carrier models. $K_{0.5}^{ee}$ is that concentration of S where the rate of equilibrium exchange transport is $V^{ee}/2$. For the simple carrier $K_{0.5}^{ee} = K^{ee}$. For two-site carriers when $R_{oo} = R_{12} + R_{21} = R_{ee}$, $K_{0.5}^{ee} = K^{ee}$.

is translocated by movement through a separate subunit. These movements are, however, coupled. Exchange transport could be slower or faster than net transport depending upon whether substrate-induced coupling is accelerative or decelerating.

A King–Altman representation of this model is shown in Figure 2B. To simplify our analysis, we assume that all substrate binding steps are rapid compared to translocation steps and that isomerization of unoccupied carrier occurs at rates significantly greater than substrate translocation (rate constants k_0 and $k_{-0} \gg k_1$ through k_{-3}). Thus binary and ternary substrate/carrier complexes are always in true equilibrium with substrate levels in the microenvironment of the carrier. At present, we have no experimental means of testing the validity of these assumptions.

As transport is passive, the following relationships must hold true:

$$\frac{k_{-0}k_1}{k_0k_{-1}} = \frac{K_1}{K_2}$$

$$\frac{k_0k_2}{k_{-0}k_{-2}} = \frac{K_3}{K_4}$$

$$\frac{k_1k_{-3}}{k_{-1}k_3} = \frac{K_8}{K_7}$$

$$\frac{k_{-0}k_3}{k_0k_{-3}} = \frac{K_1K_7}{K_2K_8}$$

$$\frac{k_1k_2}{k_{-1}k_{-2}} = \frac{K_1K_3}{K_2K_4}$$

The law of microscopic reversibility requires that $K_4K_6 = K_1K_7$ and $K_3K_5 = K_2K_8$. Tables I and II summarize the solutions to this transport model.

(*B*) *An Allosteric Two-Site Carrier.* A variant of the two-site transporter containing simultaneously existent, cis–trans substrate binding sites is shown in Figure 3A. Again, the carrier always presents substrate efflux and substrate influx sites to the surrounding media. In the absence of substrate, two substrate influx sites and two substrate efflux sites are available on the transporter. Once a substrate is bound to one of these sites, a conformational change occurs in which the second cis and the cis–trans sites are lost. Thus binding of S_2 to one uptake site results in the loss of the second (cis) uptake site and the loss of the cis–trans exit site. As with the iso-two-site model, exchange transport does not involve simultaneous movements of substrate molecules through a single internal cavity. Each molecule is translocated by coupled movement through separate subunits.

A King–Altman representation of this model is shown in Figure 3B. To simplify our analysis, we assume that all substrate binding steps are rapid with respect to translocation steps. Thus binary and ternary substrate/carrier complexes are always in true equilibrium with substrate levels in the microenvironment of the carrier. At present, we have no experimental means of testing the validity of this assumption.

As transport is passive, the following relationships must hold true:

$$\frac{k_1}{k_{-1}} = \frac{K_1}{K_2} = \frac{K_8k_3}{K_7k_{-3}}$$

$$\frac{k_2}{k_{-2}} = \frac{K_3}{K_4}$$

$$\frac{k_3}{k_{-3}} = \frac{K_1K_7}{K_2K_8}$$

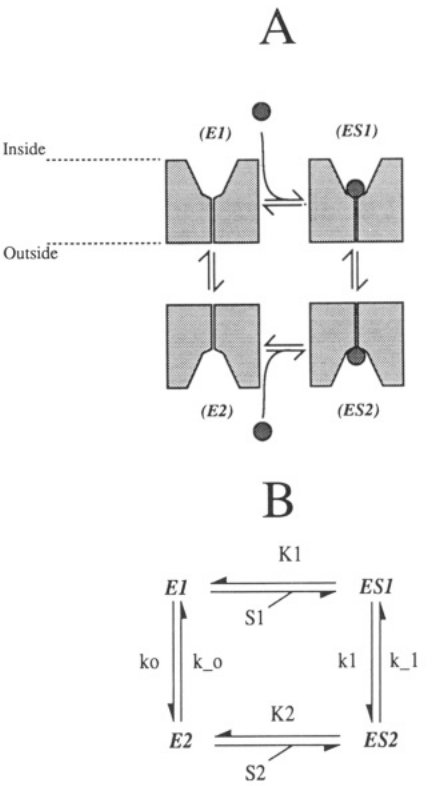

FIGURE 1: The simple carrier model for facilitated diffusion. (A) Schematic representation of the model. (B) King–Altman representation of the model. In the absence of substrate the carrier, E, can exist in one of two states: E_1, where the substrate binding site faces the cytosol, and E_2, where the substrate binding site faces the interstitium. When substrate S is present, the carrier can bind extracellular substrate (S_2) to form ES_2 or intracellular substrate (S_1) to form ES_1. Isomerizations between E_1 and E_2 states are described by the first-order rate constants k_0 and k_{-0}. Isomerizations between the ES_1 and ES_2 states are described by the first-order rate constants k_1 and k_{-1}. K_1 and K_2 are dissociation constants describing binding of S_1 to E_1 and S_2 to E_2, respectively.

The law of microscopic reversibility requires that $K_4K_6 = K_1K_7$ and $K_3K_5 = K_2K_8$. Tables I and II summarize the solutions to this transport model.

Unstirred Layers/Compartmentalization of Intracellular Sugar. Figure 4 illustrates a model in which sugars are compartmentalization within the cell. This could result either from the presence of an unstirred sugar layer just below the cell membrane or from the presence of sugar binding proteins (e.g., hemoglobin) inside the cell.

The analysis is similar to that of Naftalin et al. (1985) and Helgerson and Carruthers (1989). The system consists of three compartments. C_1^b contains the bulk intracellular sugar. C_1^m lies below the membrane and contains transporter-accessible sugar. C_2 is the extracellular compartment. Sugar exchange, J, between compartments C_1^b and C_1^m is described by the permeability coefficient D_1:

$$^{NET}J_{C_1^m \rightarrow C_1^b} = D_1(S_{C_1^m} - S_{C_1^b}) \quad (1)$$

Prior to injection of sugar-loaded cells into sugar poor medium, the concentration of intracellular sugar in compartments C_1^b and C_1^m is identical although the amount of sugar present in each compartment (N^m and N^b) of a unit number of cells is proportional to compartment size. For simplicity, the dead value of the cell is considered to be negligible (although this assumption is invalid), and water flow between compartments is assumed to be unrestricted. Upon injection of cells into sugar-poor medium an osmotic water movement into the cell occurs. The concentrations of S within compartment C_1^m (S^m)

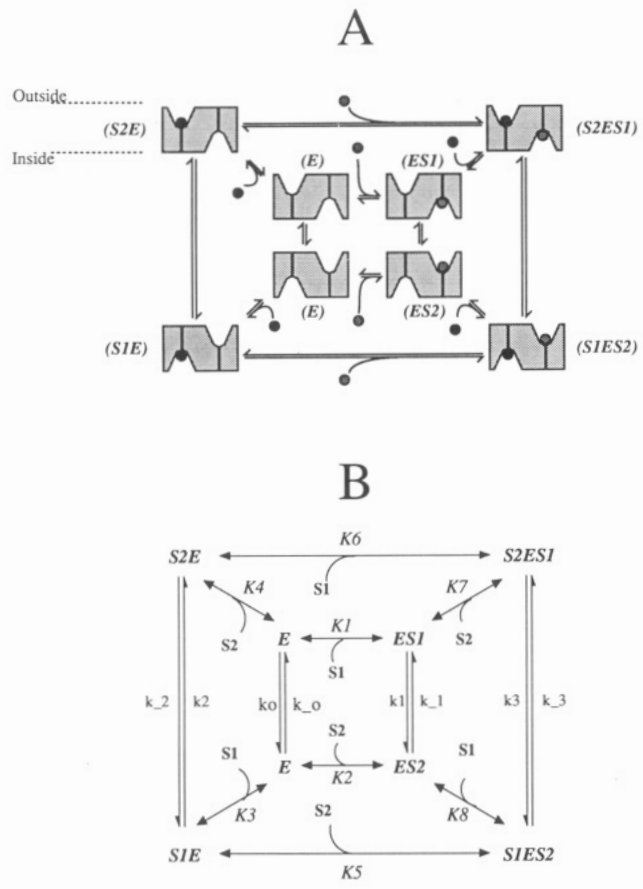

FIGURE 2: The iso-two-site model for facilitated diffusion. (A) Schematic representation of the model. (B) King–Altman representation of the model. In the absence of substrate the carrier, E, can exist in one of two possible states. Both states simultaneously present influx and efflux sites to the microenvironment surrounding the carrier. Isomerizations between these two states are described by the first-order rate constants k_0 and k_{-0}. When substrate, S, is present, the carrier can bind 2 molecules of S to form either the S_2·E·S_1 or the S_1·E·S_2 complex. Exchange transport does not involve simultaneous movements of S through a single pore but, rather, coupled movements of S through separate pores or subunits. Dissociation constants (upper case K terms) and rate constants describing isomerization rates (lower case k terms) are shown where appropriate in (B).

and of radiolabeled sugar P (P^m) in this compartment are given by

$$S^m = \frac{N_s^m}{V^m} \text{ and } P^m = \frac{N_p^m}{V^m} \quad (2)$$

where V^m is the volume of compartment $C_1{}^m$.

Similarly, the concentrations of S within compartment $C_1{}^b$ (S^b) and of radiolabeled sugar P (P^b) in this compartment are given by

$$S^b = \frac{N_s^b}{V^b} \text{ and } P^b = \frac{N_p^b}{V^b} \quad (3)$$

where V^b is the volume of compartment $C_1{}^b$. If Q is the osmolarity of osmotically active but nontransported species present in compartment C_2, N_Q^b and N_Q^m are the amount of these species present in $C_1{}^b$ and $C_1{}^m$, and S_2 and P_2 are the concentrations of unlabeled and labeled sugars at the exterior of the cell, we have at osmotic equilibium

$$V^m = \frac{N_Q^m + N_s^m + N_p^m}{Q + S_2 + P_2} \text{ and } V^b = \frac{N_Q^b + N_s^b + N_p^b}{Q + S_2 + P_2} \quad (4)$$

giving

$$S^m = \frac{N_s^m(Q + S_2 + P_2)}{N_Q^m + N_s^m + N_p^m} \text{ and } P^m = \frac{N_p^m(Q + S_2 + P_2)}{N_Q^m + N_s^m + N_p^m} \quad (5)$$

and in analogous fashion for sugar in compartment $C_1{}^b$:

$$S^b = \frac{N_s^b(Q + S_2 + P_2)}{N_Q^b + N_s^b + N_p^b} \text{ and } P^b = \frac{N_p^b(Q + S_2 + P_2)}{N_Q^b + N_s^b + N_p^b} \quad (6)$$

Explicit solutions to the transport velocity equations allowing for exchange of sugars between compartments are complex. The approach adopted was to obtain numerical solutions to the differential exchange equations (eq 7 and 8, see below) allowing for sugar exchange between intracellular compartments (eq 1) with correction for volume changes (eqs 5 and 6) using fourth-order Runge–Kutta numerical integration. Step sizes (dt) employed in simulations were reduced until further reduction was without significant effect on the computed results (dt = 1 μs).

Results

General Form of the Velocity Equations in the Absence of Unstirred Layers. The general form of the transport velocity equations is identical for all three models. According to the nomenclature of Lieb and Stein (1974b; but avoiding any physical interpretation of the derived constants), unidirectional sugar efflux (v_{12}) is described by

$$v_{12} = \frac{S_1(K + S_2)}{K^2R_{oo} + KR_{12}S_1 + KR_{21}S_2 + R_{ee}S_1S_2} \quad (7)$$

where S_1 and S_2 refer to substrate (S) concentrations at sides 1 and 2 of the membrane, respectively, and the various constants (K, R_{oo}, R_{12}, R_{21}, and R_{ee}) are described in Table I. Unidirectional substrate uptake (v_{21}) is obtained by interchanging S_1 and S_2 in the numerator of eq 7.

When labeled substrate (P) is used as a tracer for movements of S, the velocity equation is

$$v_{12}^p = \left(\frac{P_1}{K} + \frac{P_1P_2}{K^2} + \frac{P_1S_2}{K^2}\right) \Big/ \left[R_{oo} + \frac{R_{12}}{K}(S_1 + P_1) + \frac{R_{21}}{K}(S_2 + P_2) + \frac{R_{ee}}{K^2}(S_1S_2 + P_1P_2 + P_1S_2 + P_2S_1)\right] \quad (8)$$

Unidirectional labeled substrate uptake (v_{21}^p) is obtained by interchanging P_2 for P_1 and S_1 for S_2 in the numerator of eq 8. The values of the constants (K through R_{ee}) can be calculated from the experimentally determined Michaelis and velocity parameters as shown in Table II.

When S approaches zero, the rate equations reduce to an expression that is first order in substrate and in which a single pseudo-first-order rate constant, π, governs the rate. Thus

$$v = \pi S$$

where for zero-trans fluxes

$$\pi = \frac{V_{max}}{K_{m(app)}}$$

For zero-trans and equilibrium exchange transport conditions π is independent of the transport model and is described by

$$\pi = \frac{1}{R_{oo}K} \quad (9)$$

Differences between Simple and Two-Site Models. With the simple carrier, the relationship

$$R_{12} + R_{21} - R_{ee} - R_{oo} = 0 \quad (10)$$

must always hold true. Here $K^{ee} = K_{0.5}^{ee}$.

With the two-site carriers, this relationship, although possible, need not always be satisfied. In situations where eq 10

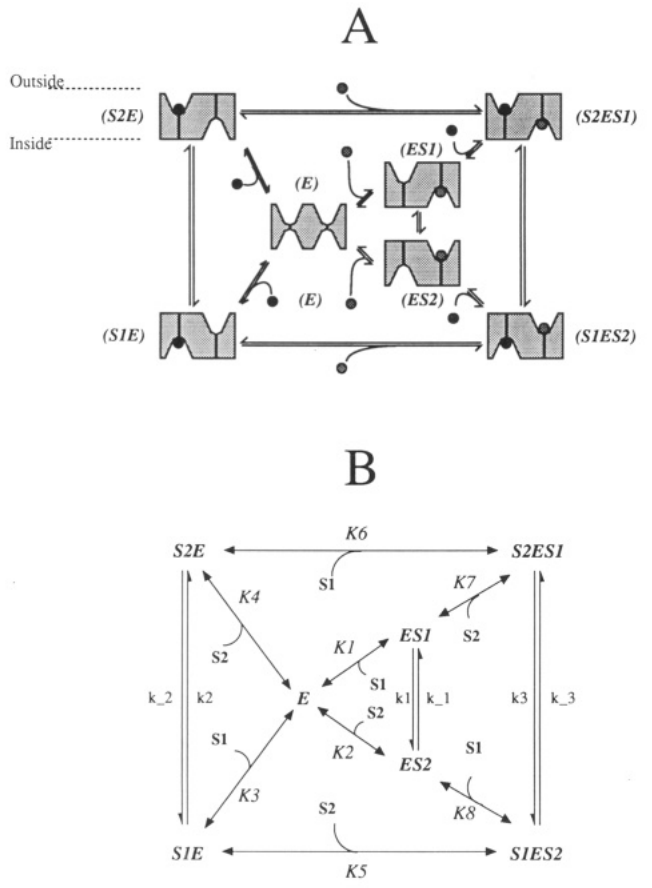

FIGURE 3: The allosteric two-site model for facilitated diffusion. (A) Schematic representation of the model. (B) King–Altman representation of the model. In the absence of substrate the carrier, E, exists in one state. E simultaneously presents two influx and two efflux sites to the microenvironment surrrounding the carrier. When one influx site is occupied by S_2, the second influx site and the cis–trans efflux site are lost. Similarly, when one efflux site is occupied by S_1, the second efflux site and the cis–trans uptake site are lost. When substrate is present at both sides of the membrane, the carrier can bind 2 molecules of S to form either the $S_2{\cdot}E{\cdot}S_1$ or the $S_1{\cdot}E{\cdot}S_2$ complex. Exchange transport does not involve simultaneous movements of S through a single pore but, rather, coupled movements of S through separate pores or subunits. Dissociation constants (upper case K terms) and rate constants describing isomerization rates (lower case k terms) are shown where appropriate in (B).

is not satisfied, the relationship between equilibrium exchange unidirectional fluxes and substrate concentration is nonhyperbolic. Equation 9 is still valid under these conditions, but π is no longer obtained as $V^{ee}/K^{ee}_{0.5}$. When eq 10 is satisfied, equilibrium exchange transport displays simple hyperbolic kinetics, and simple carrier- and two-site carrier-mediated transport are indistinguishable.

Nonhyperbolic Two-Site Carrier Equilibrium Exchange Transport. The general equation for a Hanes–Woolf analysis of equilibrium exchange data (S/v^{ee} versus S) takes the form:

$$\frac{S}{v^{ee}} = KR_{oo} + R_{ee}S + \frac{(R_{12} + R_{21} - R_{oo} - R_{ee})KS}{K + S} \qquad (11)$$

Three examples are illustrated in Figure 5, where trans acceleration of transport is observed ($R_{ee} < R_{12} = R_{21}$). When $R_{12} + R_{21} - R_{ee} - R_{oo} = 0$, the data points fall on a single straight line with y-intercept = KR_{oo} and slope = R_{ee}. In this instance, the substrate velocity data do not deviate from simple hyperbolic kinetics.

When $R_{oo} + R_{ee} > R_{12} + R_{21}$, at low S the data points fall rapidly and nonlinearly with increasing S below the value KR_{oo} and then increase linearly with S at high S. The slope of the data points at high S is R_{ee}, and the y-intercept at $S = 0$ is unchanged as KR_{oo}.

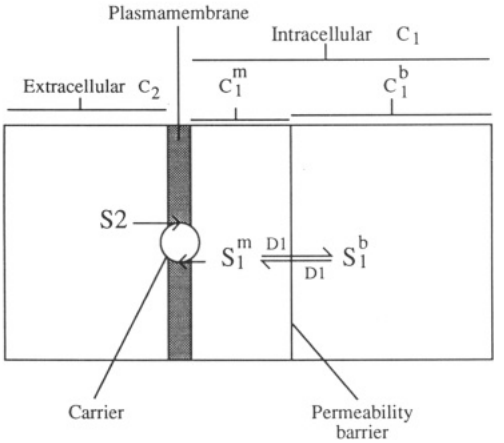

FIGURE 4: Compartmentalization of intracellular sugars. Three compartments are described: extracellular medium (C_2), intracellular subplasmalemmal compartment (C_1^m), and intracellular bulk solution (C_1^b). The glucose carrier responds only to sugars in the extracellular and C_1^m compartments. Exchange of sugar between intracellular compartments is described by the first-order rate constant D_1.

When $R_{oo} + R_{ee} < R_{12} + R_{21}$, at low S the data points increase rapidly and nonlinearly with increasing S above the value KR_{oo} and then increase linearly with S at high S. The slope of the data points at high S is R_{ee}, and the y-intercept at $S = 0$ is unchanged as KR_{oo}.

When exchange transport displays simple saturation kinetics, two parameters can be obtained from Hanes–Woolf analysis: R_{ee} (slope) and the product KR_{oo} (y-intercept). When nonhyperbolic exchange kinetics are encountered, five parameters can be obtained from Hanes–Woolf analysis: R_{ee} (slope at high S), KR_{oo} (y-value at limitingly low S), $R_{12} + R_{21}$, K, and R_{oo}. The latter three parameters are obtained directly by nonlinear regression analysis or by an indirect approach.

The indirect approach requires subtraction of the value $(KR_{oo} + SR_{ee})$ from the data points. This yields a hyperbola extending into either positive or negative S/v_{ee} space (see Figure 5) that may then be analyzed by linearization to obtain the maximum $K(R_{12} + R_{21} - R_{oo} - R_{ee})$ and the half-saturation constant K (see Figure 5). Thus for two-site carrier transport systems displaying nonhyperbolic equilibrium exchange substrate–velocity relationships, only two transparent conditions are necessary to obtain a full set of transport parameters: zero-trans uptake (to obtain R_{21}) and equilibrium exchange (to obtain R_{12}, R_{ee}, R_{oo}, and K).

Unstirred Layers/Compartmentalization of Intracellular Sugar. Sugar transport was simulated in which the intrinsic properties of the transporter satisfy eq 10 (hyperbolic kinetics are obtained under all conditions). The carrier was assumed to be symmetric ($R_{12} = R_{21}$) and to display trans acceleration ($R_{ee} < R_{12}$), and the parameters R_{12} and R_{ee} were assigned values close to those observed in human red cells at 20 °C. The size of compartment C_1^m was arbitrarily assigned a value one-ninth of that of C_1^b, and the rate constant D_1 describing exchange of sugars between these compartments was varied over the range 0.0005–100 s^{-1}. Figure 6 illustrates the effect of decreasing D_1 on infinite-cis net sugar uptake. These simulations show that it is technically unfeasible to obtain estimates of the intrinsic properties of the transport system using transport incubation intervals of 1 ms or longer even at the highest values of D_1.

Discussion

This paper describes two classes of models for the facilitated

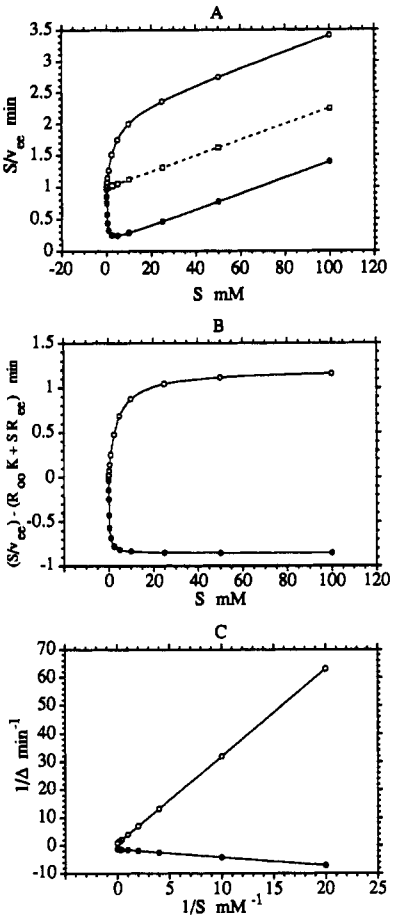

FIGURE 5: Analysis of equilibrium exchange transport data. Three types of idealized, two-site transporters are represented in this figure. In all instances trans acceleration is observed ($R_{ee} < R_{12} = R_{21}$). The simplest case is of a transporter characterized by $R_{12} + R_{21} = R_{ee} + R_{oo}$ (open squares). The second case is of a transporter characterized by $R_{12} + R_{21} > R_{ee} + R_{oo}$ (open circles). The third case is of a transporter characterized by $R_{12} + R_{21} < R_{ee} + R_{oo}$ (filled circles). (A) Hanes–Woolf analysis of equilibrium exchange data. Ordinate: S/exchange rate (v_{ee}) in min. Abscissa: S concentration. (B) Analysis of nonhyperbolic exchange transporters. The transport data points (S/v_{ee}) are adjusted for the linear components present in (A) by subtraction of $R_{oo}K$ [the y-intercept in (A)] plus SR_{ee} [the linear component of (A)]. The resulting plots are sections of rectangular hyperbolas extending into positive y-space ($R_{12} + R_{21} > R_{ee} + R_{oo}$) and negative y-space ($R_{12} + R_{21} < R_{ee} + R_{oo}$). (C) The data of (B) are linearized in the form $1/\{(S/v_{ee}) - (KR_{oo} + SR_{ee})\}$ (shown as $1/\Delta$) versus $1/S$. The resulting x-intercept of these plots corresponds to $-1/K$, and the y-intercept corresponds to $1/\{K(R_{12} + R_{21} - R_{oo} - R_{ee})\}$.

diffusion of substrate across cell membranes. These transport systems differ in the number of substrate transport sites present per carrier. The simple carrier contains only a single substrate binding site at any instant in time. This carrier exposes either an influx or an efflux site but never both simultaneously. The two-site carriers expose both influx and efflux sites simultaneously. The simple carrier and the iso-two-site carrier allow for isomerizations of carrier between two states in the absence of substrates.

The two-site carriers presented in this analysis differ from those of previous analyses (Baker & Widdas, 1973; Naftalin & Holman, 1977; Krupka & Deves, 1978) in two fundamental regards. (1) The current analysis allows explicitly for cooperativity in substrate binding. (2) The current analysis does not make the simplifying assumption of a single, central ternary complex of extracellular sugar/carrier/intracellular sugar. The major consequence of these differences is to remove the restriction of hyperbolic equilibrium exchange kinetics only

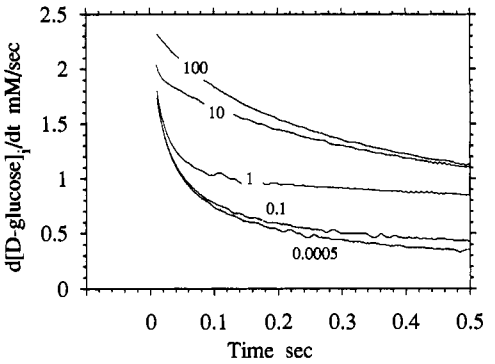

FIGURE 6: Effects of compartmentalization of intracellular glucose on the rate of D-glucose uptake. Sugar transport was simulated in which the intrinsic properties of the transporter satisfy eq 10 (hyperbolic kinetics are obtained under all conditions). The carrier was assumed to be symmetric ($R_{12} = R_{21} = 0.00666$ L of cell water·min·mmol^{-1}) and to display trans acceleration ($R_{ee} = 0.5R_{12}$) and $K = 0.333$ mM (values close to those observed in human red cells at 20 °C). The size of compartment C_1^m was arbitrarily assigned a volume one-ninth of that of C_1^b, and the rate constant D_1 describing exchange of sugars between these compartments was varied over the range 0.0005–100 s^{-1}. The time course of 100 mM D-glucose uptake was simulated by fourth-order Runge–Kutta numerical integration employing step intervals of 1 μs with corrections for volume changes (see Theory for details). Simulated uptake data were collected over 1-ms intervals. The first derivative of these data provides the instantaneous uptake rate (v or d[D-glucose]$_i$/dt) and is plotted as a function of the first 0.5 s of transport. As the rate of exchange of D-glucose between C_1^m and C_1^b (D_1, shown on each curve) is attenuated from 100 s^{-1} (uppermost curve) to 0.0005 s^{-1} (lowest curve), the estimated rate of uptake is reduced. Even at the highest value of D_1, uptake during the first millisecond of transport is underestimated.

under conditions where trans acceleration is not observed (Krupka & Deves, 1978).

The two-site carriers presented here also differ in a single fundamental way. The iso-two-site carrier allows for isomerizations of unoccupied carrier between two states whereas the allosteric two-site carrier exists in a single conformation in the absence of substrate. It is unlikely that this difference would be significant in analyses of steady-state sugar transport measurements. However, interpretation of pre-steady-state sugar transport data and of pre-steady-state, substrate-induced, glucose carrier intrinsic fluorescence quenching data is critically dependent upon the distribution of carrier conformations in the presumed mechanism of transport (Lowe & Walmsley, 1987; Naftalin, 1988; Appleman & Lienhard, 1989).

General Properties of the Transport Models. Simple carrier-mediated transport is characterized by hyperbolic (Michaelis–Menten) kinetics under all conditions. The two-site carriers are restricted to hyperbolic kinetics under all conditions save that of equilibrium exchange transport. When simple and two-site carrier systems display hyperbolic kinetics under all conditions, these classes of carrier systems are indistinguishable by analysis of steady-state transport data alone.

Krupka (1989) shows that substrate transport data may be rejected if a series of simple relationships are not satisfied. These relationships are independent of any presumed mechanism of transport but are constrained by the requirement of hyperbolic kinetics under all transport conditions (i.e., $R_{12} + R_{21} = R_{oo} + R_{ee}$). The relationships are

$$\frac{V^{ee}}{K^{ee}_{0.5}} = \frac{V^{zt}_{12}}{K^{zt}_{12}} = \frac{V^{zt}_{21}}{K^{zt}_{21}}$$

If an incomplete equilibrium exchange transport data set is obtained such that a linear transformation of the data suggests hyperbolic kinetics (e.g., as in Figure 5 at high substrate

Table III: Simple and Two-Site Analysis of Facilitated Diffusion Systems

transport system	measured transport properties: exchange/symmetry[a]	measured transport properties: relationship between R parameters[b]	modeled by: simple carrier[c]	modeled by: two-site carrier[d]	reference
sugars					
human RBC	$R_{ee} < R_{12} < R_{21}$	not determinable	?	?	Carruthers (1990)
rabbit RBC	$R_{ee} = R_{12} = R_{21}$	$R_{12} + R_{21} = R_{ee} + R_{oo}$	yes	yes	Regen and Morgan (1964)
rat RBC	$R_{ee} < R_{12} < R_{21}$	$R_{12} + R_{21} = R_{ee} + R_{oo}$	yes	yes	Whitesell et al. (1989)
	$R_{ee} < R_{12} = R_{21}$	$R_{12} + R_{21} < R_{ee} + R_{oo}$	no	yes	Helgerson and Carruthers (1989)
rat hepatocyte	$R_{ee} = R_{12} = R_{21}$	$R_{12} + R_{21} = R_{ee} + R_{oo}$	yes	yes	Craik and Morgan (1979)
rat adipocyte	$R_{ee} = R_{12} = R_{21}$	$R_{12} + R_{21} = R_{ee} + R_{oo}$	yes	yes	Taylor et al. (1981)
squid giant axon	$R_{12} < R_{21} = R_{ee}$	$R_{12} + R_{21} = R_{ee} + R_{oo}$	yes	yes	Baker and Carruthers (1981)
giant barnacle fiber	$R_{ee} = R_{12} = R_{21}$	$R_{12} + R_{21} = R_{ee} + R_{oo}$	yes	yes	Carruthers (1983)
transport of other solutes by the human RBC					
leucine	$R_{ee} < R_{12} = R_{21}$	$R_{12} + R_{21} = R_{ee} + R_{oo}$	yes	yes	Hoare (1972a,b)
uridine	$R_{ee} < R_{12} < R_{21}$	$R_{12} + R_{21} = R_{ee} + R_{oo}$	yes	yes	Cabantchik and Ginsburg (1977)
cAMP	$R_{ee} = R_{21} < R_{12}$	$R_{12} + R_{21} = R_{ee} + R_{oo}$	yes	yes	Holman (1978)

[a] Accelerated exchange is observed when $R_{ee} < R_{12}$ or $R_{ee} < R_{21}$. Decelerated exchange is observed when $R_{ee} > R_{12}$ or $R_{ee} > R_{21}$. No exchange phenomena are observed when $R_{ee} = R_{12} = R_{21}$. Transport is symmetric when $R_{12} = R_{21}$. [b] The R parameters refer to the parameters R_{12}, R_{21}, R_{ee}, and R_{oo}, which are defined in Table I. When $R_{12} + R_{21} = R_{ee} + R_{oo}$, all transport conditions display simple hyperbolic kinetics and simple and two-site carrier models cannot be distinguished. [c] Determines whether the transport data are compatible with the simple carrier. [d] Determines whether the transport data are compatible with the allosteric and iso-two-site carriers. (?) indicates that conflicting data have been reported.

concentrations), the requirement of hyperbolic kinetics will appear to be satisfied. However, if $R_{12} + R_{21} \neq R_{oo} + R_{ee}$, it will be apparent immediately that the ratio $V^{ee}/K^{ee} \neq V^{zt}/K^{zt}$. According to the rules outlined by Krupka, this must lead to rejection of one or more of the data sets. In fact, the data set may be technically sound, but the substrate concentration range employed did not extend to sufficiently low substrate levels to reveal nonhyperbolic exchange kinetics. In order to determine whether equilibrium exchange transport displays nonhyperbolic kinetics, it is important to measure transport at concentrations of substrate over the range 0.02–$0.2K^{ee}_{0.5}$.

Analysis of Facilitated Diffusion Systems. Table III presents an analysis of seven sugar transport systems displaying distinct transport properties. In almost all instances, both simple and two-site carriers are compatible with the available transport data. Uridine, leucine, and cAMP transport by human erythrocytes also falls into this general category of transport systems [see Stein (1986)], being compatible with both forms of carrier models. With these transport systems, the use of steady-state transport data alone is insufficient to distinguish between simple and two-site mechanisms for transport.

The single, anomalous transport system listed in Table III appears to be human erythrocyte hexose transfer. A recent study suggests that human erythrocyte hexose transport may be compatible with the simple carrier mechanism (and by inference compatible also with the two-site carrier mechanisms; Wheeler & Whelan, 1988) while an earlier, similar study concluded that transport was inconsistent with both models (Baker & Naftalin, 1979). Disagreements in estimates of K^{ic}_{21} and K^{it}_{12} suggest that technical problems in obtaining reliable estimates of transport constants may, in part, explain the difficulty in interpreting human red cell sugar transport data [see Carruthers (1990)].

One source of technical difficulty could arise from the presence of an unstirred layer or permeability barrier to sugar movements just below the endofacial surface of the plasma membrane (see Figure 4; Miller, 1968; Baker & Naftalin, 1979; Naftalin & Holman, 1977; Naftalin et al., 1985; Helgerson & Carruthers, 1989). The presence of such a permeability barrier would invalidate interpretation of transport constants within the context of simple and two-site mechanisms for transport. We illustrate this in the following way. Table IV and Figure 6 summarize computations of sugar uptake in which the red cell sugar carrier was simulated as a symmetric system displaying trans acceleration ($R_{12} = R_{21} = 2R_{ee}$), where $R_{12} + R_{21} - R_{oo} - R_{ee} = 0$ (hyperbolic kinetics are observed for all transport conditions) but where intracellular sugar is compartmentalized and exchange between

Table IV: Simulations of Erythrocyte Sugar Transport in the Presence of an Intracellular Unstirred Sugar Layer[a]

transport parameters: constants[b]	transport parameters: assumed intrinsic value	experimental values: Michaelis and velocity parameters[c]	experimental values: unstirred layer is absent[d]	experimental values: unstirred layer is present[e]
K	0.333	K^{zt}_{12}	0.5	8.8
R_{12}	0.00666	K^{zt}_{21}	0.5	2.1
R_{21}	0.00666	K^{ic}_{21}	0.666	3.2
R_{oo}	0.01	K^{ic}_{12}	0.666	0.65
R_{ee}	0.00333	$K^{ee}_{0.5}$	1	23.7
D_1	0.1	V^{zt}_{12}	150	174.4
C_1^m/C_1^b	0.111	V^{zt}_{21}	150	34.3
		V^{ee}	300	300
		π^{zt}	300	16.3–19.8
		π^{ee}	300	12.6

[a] Human erythrocyte sugar transport is simulated by assuming the presence or absence of an unstirred sugar layer just below the cytosolic surface of the plasma membrane (see Figure 4 and Theory for details). Experimental values refer to those obtained during the first 1 s of transport (i.e., transport measurements were made over a 1-s incubation interval). [b] These are the constants described in Tables I and II and refer to the *intrinsic* constants of the transporter. The values assigned to these constants resemble those for human erythrocyte sugar transport at 20 °C with the following arbitrary constraints. Transport is symmetric ($R_{12} = R_{21}$) and displays trans acceleration ($R_{ee} < R_{12}$). The transporter should display simple hyperbolic kinetics under all conditions ($R_{12} + R_{21} = R_{ee} + R_{oo}$). Thus transport is mediated either by a simple or two-site carrier. The K parameter has units of mM, and the R parameters have units of min·mM^{-1}. D_1 refers to the rate constant for movement of sugars across the unstirred layer (permeability barrier) and has units of s^{-1}. The ratio C_1^m/C_1^b refers to the ratio of the volumes of the unstirred layer and bulk compartments within the cell. [c] Michaelis (K), velocity (V), and first-order rate constants (π) for transport (see Table II for details). Michaelis constants have units of mM. Velocity constants have units of mmol·(L of cell water)$^{-1}$·min^{-1}, and π has units of min^{-1}. The values of these parameters were obtained by linearization (Hanes–Woolf analysis) of simulated substrate–velocity data. [d] Analysis of transport data assuming the unstirred layer is absent. These calculated Michaelis and velocity parameters reflect the intrinsic properties of the transport system. [e] Analysis of transport data assuming the unstirred layer is present. Note that transport now appears to be asymmetric ($R_{12} < R_{21}$) and that the π parameters are seriously underestimated.

subplasmalemmal and bulk cytosolic compartments is restrictive.

While these simulations assume arbitrary values for the various parameters, they mimic qualitatively the sugar transport properties of the red cell. That is, transport appears to be asymmetric ($R_{12} < R_{21}$) in spite of the fact that the transport system is intrinsically symmetric. They further show the need to obtain submillisecond resolution of transport rates at 20 °C in order to describe the intrinsic properties of the transport system when intracellular sugar is compartmentalized.

Evidence for a permeability barrier ($D_1 = 0.0005\ s^{-1}$) to movements of sugars inside rat erythrocytes has been described previously (Helgerson & Carruthers, 1989), and nonuniform distributions of D-glucose inside human red cells have also been noted (Naftalin et al., 1985). Whether these findings result from associations of intracellular sugar with hemoglobin (Naftalin & Holman, 1977; Bolli et al., 1982; Gillery et al., 1982; Ink et al., 1982; Irzhakh, 1988; Krishnamoorthy et al., 1983; Kumar et al., 1985; Mortensen & Brahm, 1985; Mortensen & Christophersen, 1983; Shapiro et al., 1979; Widness et al., 1980) or from the presence of an unstirred glucose layer below the plasma membrane remains to be resolved.

General Conclusions. The general form of the velocity equations for simple and two-site carrier-mediated substrate transport is identical although explicit solutions for these transport systems are model-dependent. If the steady-state substrate transport properties of a cell are consistent with the predictions of the simple carrier, they must also be consistent with the predictions of the two-site carrier models. Unlike the simple carrier, two-site carrier-mediated equilibrium exchange substrate transport is not restricted to simple hyperbolic kinetics. Under conditions where substrate levels approach zero, zero-trans and equilibrium exchange transport are characterized by first-order kinetics in which the first-order rate constants are identical for both conditions. However, for nonhyperbolic, two-site equilibrium exchange transport, this rate constant is not described by $V^{ee}/K^{ee}_{0.5}$. In cells possessing high substrate transport capacity (e.g., human erythrocyte sugar transport), the presence of unstirred substrate layers inside the cell may require the use of submillisecond incubation intervals to reveal the intrinsic kinetic features of the transport system.

In instances where substrate transport displays simple hyperbolic kinetics under all conditions, we conclude that the use of simple, steady-state transport data alone is insufficient to characterize the mechanism of transport. Other approaches such as the analysis of transport in the presence of transport inhibitors (Krupka & Devês, 1981) are necessary.

Registry No. cAMP, 60-92-4; L-Leu, 61-90-5; uridine, 58-96-8; glucose, 50-99-7.

References

Appleman, J. R., & Lienhard, G. E. (1989) *Biochemistry 28*, 8221–8227.

Baker, G. F., & Widdas, W. F. (1973) *J. Physiol. (London) 231*, 143–165.

Baker, G. F., & Naftalin, R. J. (1979) *Biochim. Biophys. Acta 550*, 474–484.

Baker, P. F., & Carruthers, A. (1981) *J. Physiol. 316*, 481–502.

Bolli, G., Cartechini, M. G., Compagnucci, P., De, F. P., Santeusanio, F., & Brunetti, P. (1982) *Diabete Metab. 8*, 21–27.

Cabantchik, Z. I., & Ginsburg, H. (1977) *J. Gen. Physiol. 69*, 75–96.

Carruthers, A. (1983) *J. Physiol. (London) 336*, 377–396.

Carruthers, A. (1990) *Physiol. Rev. 70*, 1135–1176.

Craik, J. D., & Elliot, K. R. F. (1979) *Biochem. J. 182*, 503–508.

Deves, R., & Krupka, R. M. (1978) *Biochim. Biophys. Acta 513*, 156–172.

Gillery, P., Maquart, F. X., Gattegno, L., Randoux, A., Cornillot, P., & Borel, J. P. (1982) *Diabetes*, 371–374.

Helgerson, A. L., & Carruthers, A. (1989) *Biochemistry 28*, 4580–4594.

Helgerson, A. L., Hebert, D. N., Naderi, S., & Carruthers, A. (1989) *Biochemistry 28*, 6410–6417.

Hoare, D. G. (1972a) *J. Physiol. (London) 221*, 311–331.

Hoare, D. G. (1972b) *J. Physiol. (London) 221*, 332–348.

Holman, G. D. (1978) *Biochim. Biophys. Acta 508*, 174–183.

Holman, G. D. (1980) *Biochim. Biophys. Acta 649*, 202–213.

Holman, G. D., Busza, A. L., Pierce, E. J., & Rees, W. D. (1981) *Biochim. Biophys. Acta 649*, 503–514.

Ink, S. L., Mehansho, H., & Henderson, L. M. (1982) *J. Biol. Chem. 257*, 4753–4757.

Irzhakh, L. I. (1988) *Fiziol. Zh. SSSR im. I. M. Sechenova 74*, 564–568.

Krishamoorthy, R., Cahour, A., Elion, J., Hartmann, L., & Labie, D. (1983) *Eur. J. Biochem. 132*, 345–350.

Krupka, R. M. (1989) *Biochem. J. 260*, 885–891.

Krupka, R. M., & Devês, R. (1981) *J. Biol. Chem. 256*, 5410–5416.

Kumar, A., Sharma, K. K., & Pattabiraman, T. N. (1985) *Biochem. Med. 34*, 112–119.

Lieb, W. R., & Stein, W. D. (1974a) *Biochim. Biophys. Acta 373*, 178–196.

Lieb, W. R., & Stein, W. D. (1974b) *Biochim. Biophys. Acta 373*, 165–177.

Lowe, A. G., & Walmsley, A. R. (1986) *Biochim. Biophys. Acta 857*, 146–154.

Lowe, A. G., & Walmsley, A. R. (1987) *Biochim. Biophys. Acta 903*, 547–550.

Miller, D. M. (1968) *Biophys. J. 8*, 1339–1352.

Mortensen, H. B., & Christophersen, C. (1983) *Diabete Metab. 9*, 232–232.

Mortensen, H. B., & Brahm, J. (1985) *Clin. Chem. 31*, 1387–1389.

Naftalin, R. J. (1988) *Biochim. Biophys. Acta 946*, 431–438.

Naftalin, R. J., & Holman, G. D. (1977) *Membr. Transp. Red Cells*, 257–300.

Naftalin, R. J., Smith, P. M., & Roselaar, S. E. (1985) *Biochim. Biophys. Acta 820*, 235–249.

Regen, D. M., & Morgan, H. E. (1964) *Biochim. Biophys. Acta 79*, 151–166.

Shapiro, R., McManus, M., Garrick, L., McDonald, M. J., & Bunn, H. F. (1979) *Metabolism*, 427–430.

Stein, W. D. (1986) in *Transport and Diffusion across Cell Membranes*, pp 231–305, Academic Press, New York.

Taylor, L. P., & Holman, G. D. (1981) *Biochim. Biophys. Acta 642*, 325–335.

Wheeler, T. J., & Whelan, J. D. (1988) *Biochemistry 27*, 1441–1446.

Whitesell, R. R., Regen, D. M., Beth, A. H., Pelletier, D. K., & Abumrad, N. A. (1989) *Biochemistry 28*, 5618–5625.

Widdas, W. F. (1952) *J. Physiol. (London) 118*, 23–39.

Widness, J. A., Rogler, B. T., McCormick, K. L., Petzold, K. S., Susa, J. B., Schwartz, H. C., & Schwartz, R. (1980) *J. Lab. Clin. Med. 95*, 386–394.